Trimethyl Phosphate−Water Interaction: A Matrix-Isolation Infrared and ab Initio Study

K. Sankaran, V. Vidya, and K. S. Viswanathan*

Materials Chemistry Division, Chemical Group, Indira Gandhi Centre for Atomic Research, Kalpakkam 603 102, India

Lisa George and Surjit Singh†

Regional Sophisticated Instrumentation Centre, Indian Institute of Technology, Chennai 600 032, India

Received: October 14, 1997; In Final Form: January 7, 1998

Trimethyl phosphate (TMP) and water were co-deposited in nitrogen and argon matrices, and adducts of these species were identified using infrared spectroscopy. Formation of the adducts was evidenced by shifts in the vibrational frequencies of TMP and water. We computed the structures of these adducts and the vibrational frequencies at the HF/6-31G** level. The computed vibrational frequencies in the adducts involving the TMP submolecule compared well with the observed frequencies, while the agreement was rather poor for the modes involving the H_2O submolecule. Both experimental and computational studies indicated that two types of TMP−water complexes were formed: one in which the hydrogen in water was bonded to the phosphoryl oxygen of TMP and another in which the bonding was at the alkoxy oxygen of the phosphate. The stabilization energy of these adducts, corrected for zero-point energies and basis set superposition errors, was computed at both the HF/6-31G**//HF/6-31G** and MP2/6-31G**//HF/6-31G** levels. Our computations indicated that both the phosphoryl and alkoxy oxygen bonded TMP−H_2O complexes had a cyclic structure determined by a combination of two hydrogen-bonded interactions, one involving a hydrogen in water and another involving a hydrogen in the methyl group of TMP.

Introduction

The study of hydrogen-bonded complexes, both experimental and theoretical, are of considerable interest. There are a number of studies reported in the literature involving oxygen, nitrogen, and sulfur bases.[1−7] Studies on hydrogen-bonded complexes involving organic phosphates assume significance for a variety of reasons. Organic phosphates serve as model systems for understanding biological processes. Organic phosphates also have industrial applications, as extractants in a number of solvent extraction processes.

In recent works, we have studied the spectroscopy of trimethyl phosphate (TMP) and triethyl phosphate (TEP) and some of their complexes, trapped in argon and nitrogen matrices.[8−10] In this paper, we present our results on the experimental and computational studies on the complexes of TMP and H_2O. As we had reported in earlier works, TMP exists in two different conformations, having C_3 and C_1 symmetries, with the C_3 conformer being lower in energy relative to the C_1.[11,12] Furthermore, TMP offers two sites for interaction with H_2O: the phosphoryl and alkoxy oxygen. The multiplicity of conformations and sites of attack in TMP makes the TMP−H_2O system an interesting case study in hydrogen bonding.

Experimental Section

Matrix isolation experiments were carried out using a Leybold AG closed-cycle helium cryostat. The experimental technique and apparatus used in these experiments have been discussed in detail elsewhere.[8] Nitrogen, which was used as the matrix gas, and the vapors of the sample streamed out through three separate nozzles, and were deposited on a KBr substrate. The substrate temperature was maintained at 12.0 ± 0.5 K.

We used nitrogen as the matrix gas in preference to argon, since the infrared spectra of TMP trapped in nitrogen were simpler and relatively free from matrix site effects than that observed in argon.[8] We did, however, perform a few experiments in argon, the reasons for which will be discussed later.

TMP (E-Merck) was dried over P_2O_5 and distilled under reduced pressure before use. Distilled, deionized water (18 MΩ) obtained with a Milli-Q system (Millipore) was used. D_2O (E-Merck) was used without further purification. All the samples were subjected to several freeze−thaw cycles before use.

Sample-to-matrix ratios were varied over the range 1:0.06:6000 to 1:0.5:6000 (TMP:H_2O:N_2). A few experiments were also conducted using D_2O. After depositing the matrix, spectra were recorded using a BOMEM MB 100 FTIR, at a resolution of 1 cm^{-1}, covering the spectral region 4000−400 cm^{-1}. After recording a spectrum, the matrix was warmed to 35 K, maintained at this temperature for 15 min, and then recooled to 12 K. The spectrum of the matrix thus annealed was then recorded. Unless otherwise stated, all spectra shown in this paper are those recorded after annealing the matrix.

Experiments were also performed where H_2O alone was deposited in the matrix to confirm that all the product features discussed in this work did indeed involve both TMP and H_2O. Experiments in which TMP alone was deposited were also performed. Unfortunately, in all these experiments, H_2O was an inevitable impurity. However, the dependence of the intensity of the product features on the H_2O concentration confirmed the participation of both TMP and H_2O in complex formation.

* To whom correspondence should be sent (E-mail: vish@igcar.ernet.in).
† Deceased September 6, 1997.

S1089-5639(97)03333-1 CCC: $15.00
Published on Web 04/07/1998

While most of the experiments were conducted using the commonly used effusive source to deposit the matrix, a few experiments were done using a pulsed supersonic jet source. The supersonic jet source was used to prepare the complexes in the gas phase during expansion; the complexes thus prepared were then trapped on a KBr substrate along with N_2. Nitrogen was used both as the expansion gas and as the matrix. A pulsed source was used to reduce the gas load on the cryotip so that it does not suffer an excessive temperature rise. An excessive temperature rise had to be prevented to ensure that the complexes trapped in the matrix were predominantly those prepared in the expansion and not those produced due to the annealing of the matrix during deposition. In an earlier work we had used this home-built pulsed supersonic jet source to achieve conformational cooling in TMP.[11]

Computational Method

Ab initio computations on the TMP−H_2O system were performed using the Gaussian 92 program on a Hewlett-Packard Workstation (Model 715/64).[13] At the outset, using an STO-3G* basis, we carried out an extensive search of the TMP−H_2O potential surface, to locate structures corresponding to minima. In these computations, all molecular and intermolecular parameters defining the TMP−H_2O complexes were left free for optimization. Structures of TMP and H_2O were first individually optimized; these structures were used as starting geometries for optimization of the supermolecule geometry. The optimized structures of the adducts obtained at the STO-3G* level, were then used as initial geometries for optimization at the HF/6-31G** level. The 6-31G** basis was particularly chosen, since it has been shown to reproduce hydrogen bonding fairly accurately.[2] Various properties of the adducts, such as energy, vibrational frequencies, and dipole moments, were computed at the HF/6-31G** level. To obtain the stabilization energy of the adducts, we also performed single-point energy calculations at the MP2 level, using the geometries optimized at the HF/6-31G** level. The stabilization energies of the hydrogen-bonded adducts calculated at both the HF and MP2 levels were corrected for zero-point energies (ZPE) and basis set superposition errors (BSSE) using the counterpoise correction scheme outlined by Boys and Bernardi.[14]

Vibrational frequency calculations were performed to enable a detailed assignment of our experimental spectral features. Frequency calculations also helped to ascertain that the structures of the complexes that we obtained following the optimization procedure did indeed correspond to a minimum, by ensuring that all the frequencies were positive. In these complexes, the smallest frequency was ≈15 cm^{-1}.

Results

P═O Stretching Region. As reported earlier,[8] the P═O stretch of TMP in a nitrogen matrix was observed at 1287 and near 1305 cm^{-1}, with the latter occurring as a doublet (Figure 1). Recent supersonic jet-matrix isolation work[11] and ab initio computations[12] led to the assignment of the 1287 cm^{-1} feature to the P═O stretch in TMP with a C_3 conformation, while the 1305 cm^{-1} doublet was attributed to the same vibrational mode in the C_1 conformer. We believe that the 1305 cm^{-1} feature occurs as a doublet due to multiple site effects.

When TMP was co-deposited with water and the matrix then annealed, new features appeared at 1262 and 1292 cm^{-1} (Figure 1). These peaks gained in intensity as the concentration of H_2O in the matrix was increased, thus confirming that these spectral features were due to the TMP−H_2O adducts. In these experiments, the ratio of TMP:H_2O:N_2 was varied from 1:0.06:6000 to 1:0.5:6000. We observed spectral features due to the TMP−H_2O complex even when no water was deliberately introduced. This observation is not surprising, because water is an inevitable impurity in any matrix isolation experiment. As the features due to the complex were observed even at very low concentrations of TMP and H_2O in the matrix, they can be attributed to the 1:1 complex of TMP−H_2O.

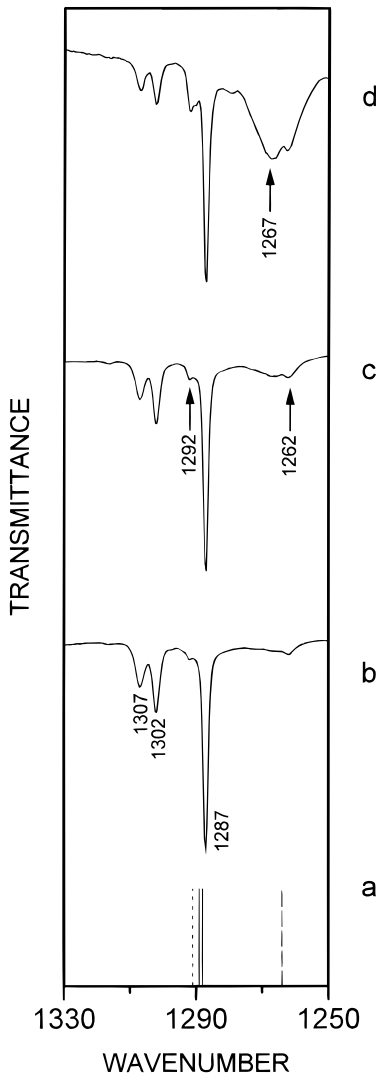

Figure 1. Matrix isolation infrared spectra in the region 1330−1250 cm^{-1}: (a) computed stick spectra; (b) TMP/N_2 (1:6000); (c) TMP/H_2O/N_2 (1:0.06:6000); (d) TMP/H_2O/N_2 (1:0.5:6000). In the stick spectra, solid lines denote features of TMP(C_1)−H_2O phosphoryl complex, long dashes TMP(C_3)−H_2O phosphoryl complex, and short dashes TMP(C_3)−H_2O alkoxy complex.

When the concentration of H_2O was increased to 1:0.5:6000 (TMP:H_2O:N_2), in addition to the above-mentioned features, we also observed a peak at 1267 cm^{-1}. As the intensity of the 1267 cm^{-1} feature increased relative to the 1262 cm^{-1} feature with increasing H_2O concentration, it is likely that this feature is due to a 1:2 adduct of TMP−H_2O. In this paper, we confine our discussion to the 1:1 complexes of TMP−H_2O and will therefore not address the problem of 1:2 adducts any further.

(P−O)−C Stretching Region. This mode occurs as a doubly degenerate mode at 866 cm^{-1} in the C_3 conformer and occurs split, at 862 and 851 cm^{-1}, in the C_1 conformer of uncomplexed TMP.[11,12] In experiments where TMP and H_2O were co-deposited, new features appeared at 870 and 857 cm^{-1} (Figure

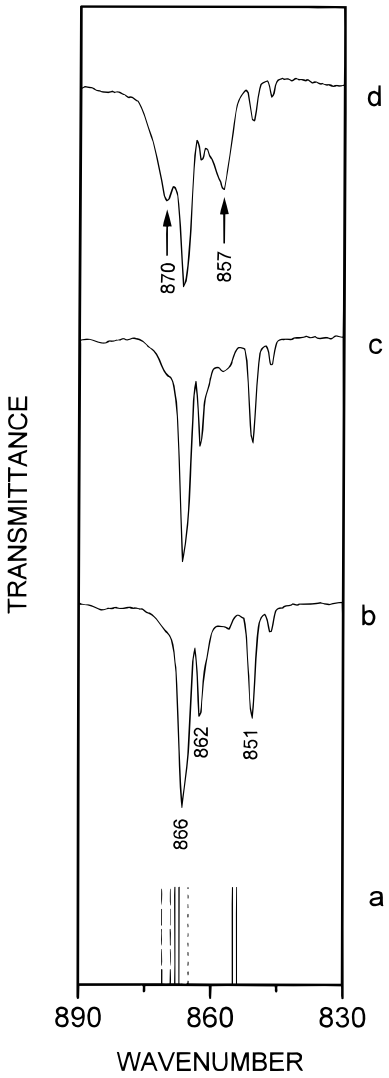

Figure 2. Matrix isolation infrared spectra in the region 890−830 cm^{-1}: (a) computed stick spectra; (b) TMP/N_2 (1:6000); (c) TMP/H_2O/N_2 (1:0.06:6000); (d) TMP/H_2O/N_2 (1:0.5:6000).

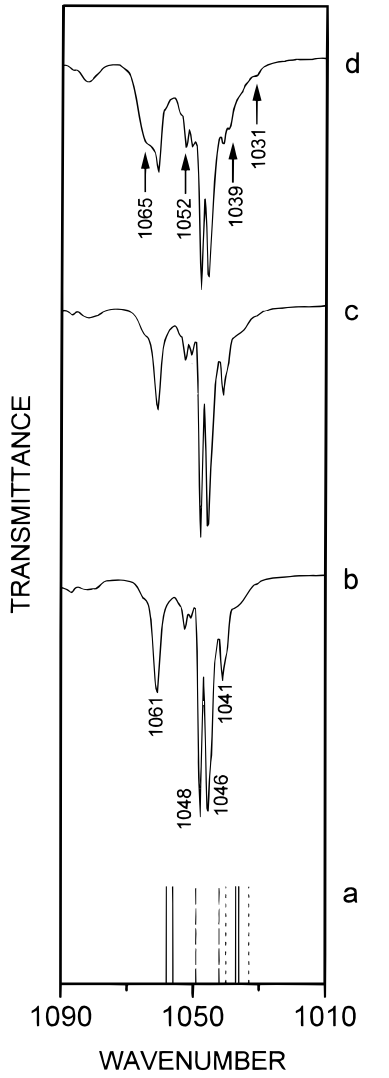

Figure 3. Matrix isolation infrared spectra in the region 1090−1010 cm^{-1}: (a) computed stick spectra; (b) TMP/N_2 (1:6000); (c) TMP/H_2O/N_2 (1:0.06:6000); (d) TMP/H_2O/N_2 (1:0.5:6000).

2), which are assigned to the (P−O)−C stretch in the TMP submolecule in the 1:1 TMP−H_2O complex.

P−(O−C) Stretching Region. This stretching mode appears in the C_3 conformer of TMP as a site-split doublet, at 1048 and 1046 cm^{-1}.[11,12] The same mode occurs in the C_1 conformer at 1061 and 1041 cm^{-1}. In our co-deposition experiments, spectral features appeared at 1031, 1039, 1050, 1052, and 1065 cm^{-1} (Figure 3). These features are assigned to the P−(O−C) stretching mode in the TMP submolecule in the 1:1 TMP−H_2O complex.

O−H Stretching Region of H_2O. The O−H stretching frequencies for monomeric H_2O occurs at 3727 (ν_3) and 3635 cm^{-1} (ν_1) in the nitrogen matrix.[15] In addition to the above-mentioned spectral features, we also observed, particularly at high H_2O concentrations, features due to the water dimer and multimers, which agreed with those reported in the literature.[15,16] When TMP and H_2O were co-deposited, we observed new features at 3460 and 3470 cm^{-1} (Figure 4), which can be assigned to the stretching mode of the H_2O submolecule in the TMP−H_2O complexes. In addition to these features, we also observed a number of weak features at 3485, 3495, 3501, and 3512 cm^{-1}. We will refer to these weak features collectively as "secondary" features. As mentioned earlier, the product features appeared even when no water was deliberately introduced in the matrix, since water is an inevitable impurity. However, these features appeared *only* when the matrix was annealed, justifying their assignment to the TMP−H_2O complexes. Furthermore, these features were observed even at low concentrations of H_2O and TMP; hence, it is reasonable to assume that all of these features were due to 1:1 complexes of TMP−H_2O. However, the large number of peaks that we observed was surprising, which warranted a detailed study.

We performed a few experiments using argon as the matrix, where only three features, at 3470, 3452, and 3442 cm^{-1}, were observed. The "secondary" features in the nitrogen matrix, observed in the region 3485−3520 cm^{-1}, were absent in the argon matrix. This observation suggests, though does not prove, the possibility that the "secondary" features may be due to stable complexes trapped in multiple sites in the nitrogen matrix.

Alternatively, the "secondary" features may be due to TMP−H_2O complexes not representing minima on the potential surface but corresponding to distorted and less stable complexes trapped in the matrix. A similar observation had been made earlier by Han and Kim.[2] They observed two spectral features that they assigned to 1:1 complexes of acetone−methanol. They attributed one of these features to a complex corresponding to a minimum they obtained in their computations. The other feature was attributed to a complex corresponding not to a stationary

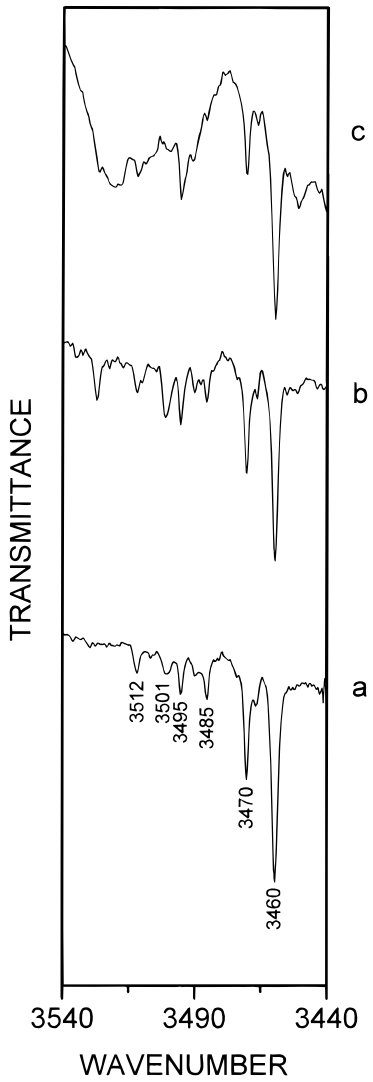

Figure 4. Matrix isolation infrared spectra in the region 3540−3440 cm^{-1}; (a) TMP/N_2 (1:6000); (b) TMP/H_2O/N_2 (1:0.06:6000); (c) TMP/H_2O/N_2 (1:0.5:6000).

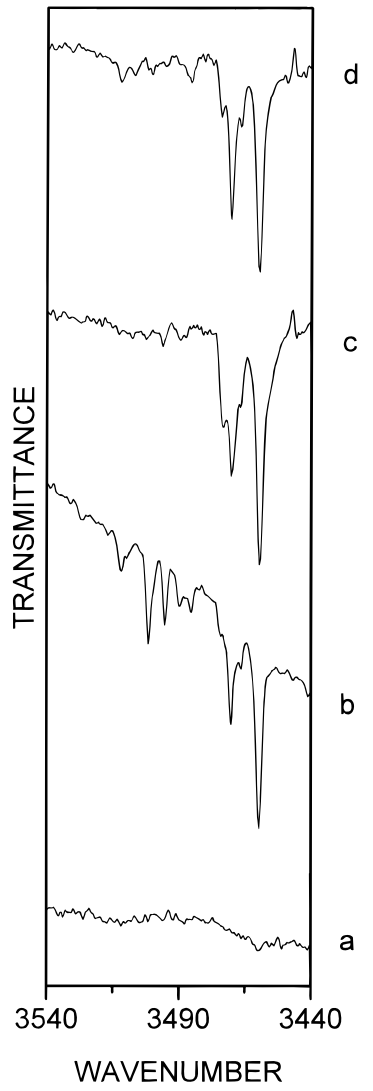

Figure 5. Comparison of matrix isolation infrared spectra of TMP/H_2O/N_2, in the region 3540−3440 cm^{-1}, obtained using an effusive and a supersonic jet source; (a) effusive source, before annealing; (b) effusive source after annealing; (c) supersonic jet source, before annealing; (d) supersonic jet source, after annealing.

point on the potential surface but to a structure with somewhat different angular intermolecular parameters compared with the stable structure. It is likely that this less stable distorted structure is stabilized by matrix interactions.

To probe the possibility that the "secondary" features may be due to such distorted complexes, we used our newly constructed pulsed supersonic jet-matrix isolation system. The logic in these experiments was as follows. If the "secondary" features were due to less stable distorted structures stabilized due to matrix interactions, then such structures should not be present if the TMP−H_2O complexes were to be produced in the gas phase. TMP−H_2O mixtures in ≈1000 Torr of N_2 were expanded through a supersonic nozzle to produce TMP−H_2O complexes, and the expanded gas mixture was then deposited on the KBr substrate mounted on the cryotip. In these experiments, N_2 served as both the expansion gas and the matrix. Adducts of TMP−H_2O were observed in these experiments (Figure 5c), even before annealing of the matrix, indicating that the adducts were formed in the supersonic expansion. (When effusive sources are used for matrix isolation experiments, annealing must be resorted to, to produce the adducts as can be seen in Figure 5a,b.) It is clear from Figure 5c that when the supersonic sampler was used, the secondary features had significantly smaller intensities than those observed in experiments where the effusive source was used. If the "secondary" features were due to stable complexes in multiple trapping sites, they should have appeared in our supersonic jet-matrix isolation experiments, with intensities comparable to that obtained in our effusive source experiments. When the matrix deposited using the supersonic jet was now annealed, the "secondary" features again picked up in intensity (Figure 5d).

We therefore believe that the weak "secondary" features may be due to distorted complexes produced during annealing. While Han and Kim proposed the formation of such complexes in the matrix based on computations, our conclusions follow from experimental considerations. We had earlier demonstrated the supersonic jet-matrix isolation technique to be a useful tool in the study of conformations; it now appears to us that the supersonic jet source can be used to address problems of matrix interaction.

Interestingly, the formation of these distorted complexes leaves no discernible signatures in the spectral regions corresponding to the TMP vibrations. Similar observations were made by Han and Kim.[2]

We do not have an explanation as to why the "secondary" features were not observed in the Ar matrix, except to say that

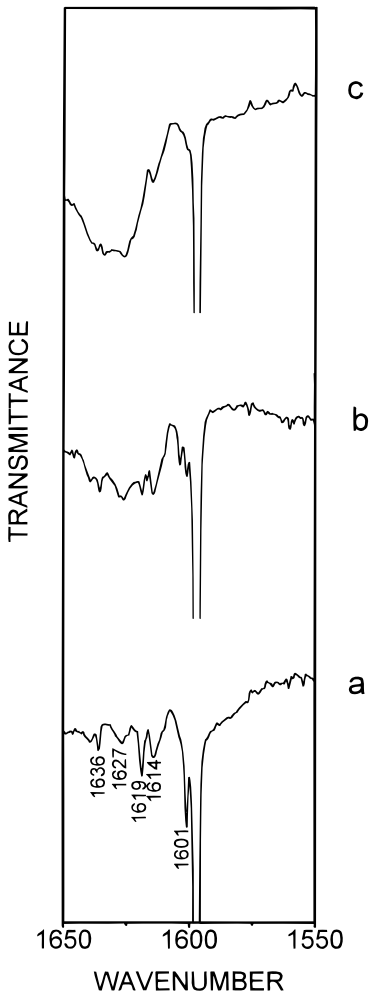

Figure 6. Matrix isolation infrared spectra in the region 1650−1550 cm^{-1}; (a) TMP/N_2 (1:6000); (b) TMP/H_2O/N_2 (1:0.06:6000); (c) TMP/H_2O/N_2 (1:0.5:6000).

Ar does not stabilize these less stable complexes. This observation does not imply that the matrix interactions in nitrogen are terribly stronger than in Ar, as to invalidate all our experimental observations. The occurrence of the main features for the O−H stretch near 3470 cm^{-1}, in both N_2 and Ar implies that the stable complexes of TMP−H_2O experience similar perturbations, if any, in both matrices.

We will henceforth consider only the features at 3460 and 3470 cm^{-1} when discussing the perturbations in the modes of H_2O in the TMP−H_2O complexes. These features can be assigned to the ν_1 stretch of H_2O in the complex, which implies that this mode is shifted by ≈170 cm^{-1}, from that observed in uncomplexed H_2O. The ν_3 mode of H_2O in the complex could not be discerned, since this mode is probably overlapped with the features due to the self-associated complexes of H_2O.

O−H Bending Region of H_2O. The bending mode (ν_2) of monomeric H_2O occurs at 1597 cm^{-1} in the nitrogen matrix. In addition to this feature we also observed the bending mode for the H_2O dimer at 1600 cm^{-1} in agreement with the literature values.[16] In addition to the features mentioned above, we also observed new bands at 1614, 1619, 1627, and 1636 cm^{-1}, when TMP and H_2O were co-deposited (Figure 6). Of these, only the 1619 cm^{-1} feature survived in the supersonic jet-matrix isolation experiment. Following a line of argument adopted in the discussion of the O−H stretching features, we deduce that the 1619 cm^{-1} feature corresponds to a stable complex that can be assigned to the ν_2 mode of the H_2O submolecule in the complex. The 1614, 1627, and 1636 cm^{-1} features, we believe, are the corresponding bending modes for the weak "secondary" features observed in the stretching region. The assignment of the 1619 cm^{-1} to the bending mode of H_2O in the complex implies a blue shift of 22 cm^{-1} relative to the frequency of this mode in uncomplexed H_2O.

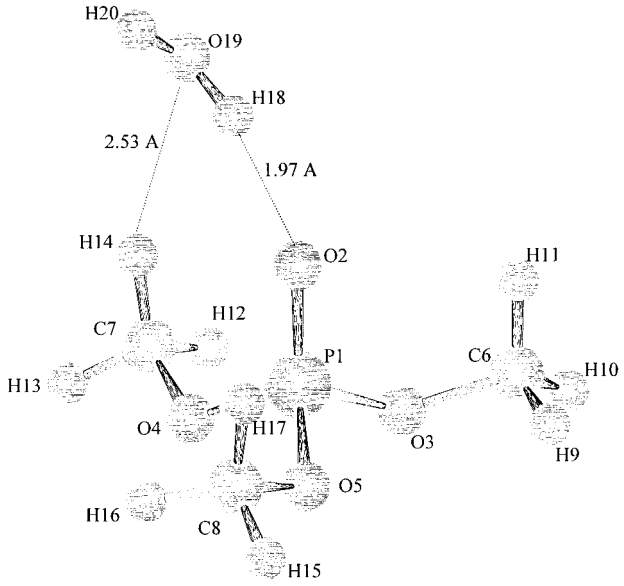

Figure 7. Structure of the TMP(C_3)−H_2O phosphoryl complex, showing selected bond distances.

Computations

Structure of the TMP−H_2O Complexes. As mentioned earlier, there are two possible hydrogen bonding sites in TMP. Our computations indicated that two types of TMP−H_2O complexes could be formed: one in which the H_2O bonds to the *phosphoryl oxygen* and another in which the bonding is at the *alkoxy oxygen* of TMP. The structures of these complexes are shown in Figures 7−9. The atom numbering indicated in these figures will be used in all subsequent discussions. The relevant structural parameters defining the complexes are shown in Table 1. Vibrational frequency calculations ensured that these structures corresponded to minima on the potential surface.

TMP(C_3)−H_2O Phosphoryl Complex. We will first discuss the structure of the complex involving the TMP submolecule with a C_3 symmetry where the H_2O was bonded to the phosphoryl oxygen. We shall denote this complex as TMP-(C_3)−H_2O phosphoryl complex, the structure of which is shown in Figure 7. The hydrogen of H_2O (H18) was located at a distance of 1.97 Å from the phosphoryl oxygen, O2. This distance is typical of most hydrogen-bonded complexes.[2−4] The H18−O2−P1 angle was ≈130° and the O19−H18−O2 angle was ≈165°, indicating a bent hydrogen bond.

In addition to the interaction of the hydrogen in water with the phosphoryl oxygen, our computations also indicated another interaction in this complex involving the methyl hydrogens in TMP. The oxygen in water (O19) was located at a distance of 2.53 Å from one of the hydrogens (H14) of the methyl group in TMP. This distance is less than the sum of the van der Waals radii of hydrogen and oxygen, indicating a possible interaction between these two atoms (O19−H14). The possibility of this interaction was further reinforced when we note that the charge density on H14 was significantly greater than in uncomplexed TMP. The charge densities on the other methyl hydrogens not involved in this interaction were insignificantly altered in the

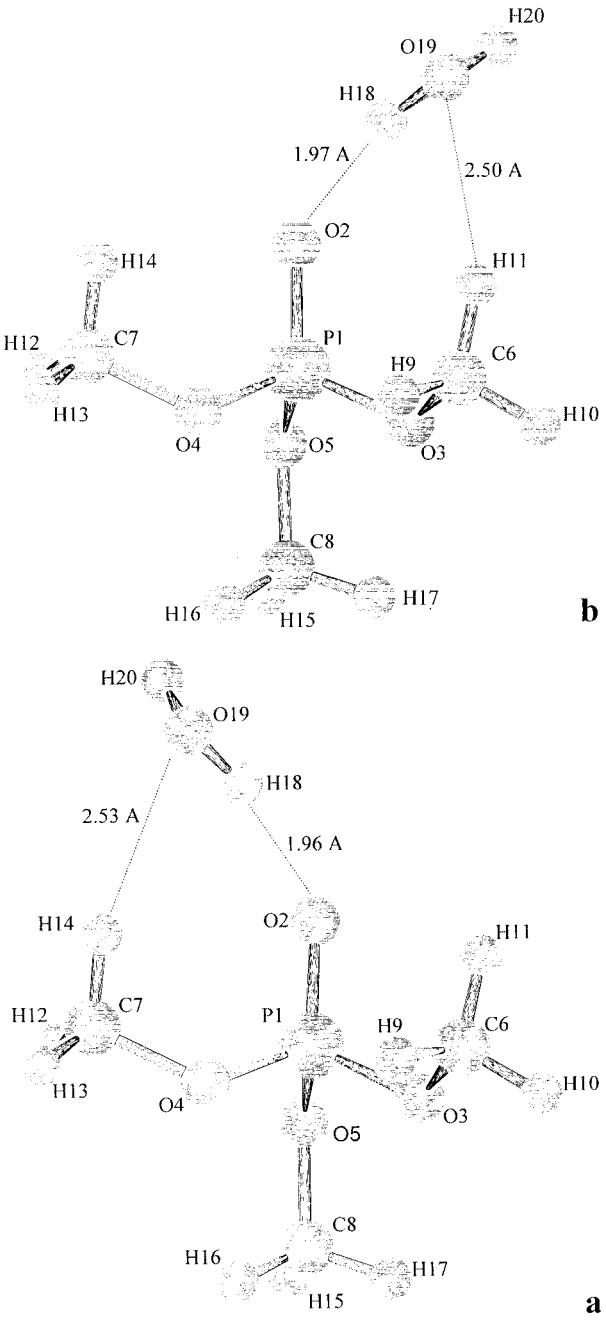

Figure 8. Structures of the TMP(C_1)−H_2O phosphoryl complexes showing selected bond distances. (a) TMP(C_1)−H_2O (I) complex; (b) TMP(C_1)−H_2O (II) complex.

complex. Furthermore, the carbon atom, C7, attached to H14, also showed a significant change in charge density, unlike the other carbon atoms, C6 and C8. Table 2 gives the charge densities on all the atoms in the complex, with the corresponding values in the uncomplexed molecules in parentheses. The numbers that reflect large changes in charge density when the complexes were formed are highlighted in bold. Of course, the scene of the stronger interaction, P═O···H−O−H, also reflect notable changes in charge density during complex formation.

It therefore appears that the structure of the complex is determined *both* by interactions involving the phosphoryl group and possibly weak interactions involving the methyl hydrogen. Similar cyclic structures involving dual interactions have also been proposed in complexes of acetone−water, acetone−methanol, and hydroxyurea−water complexes. [2,3,17]

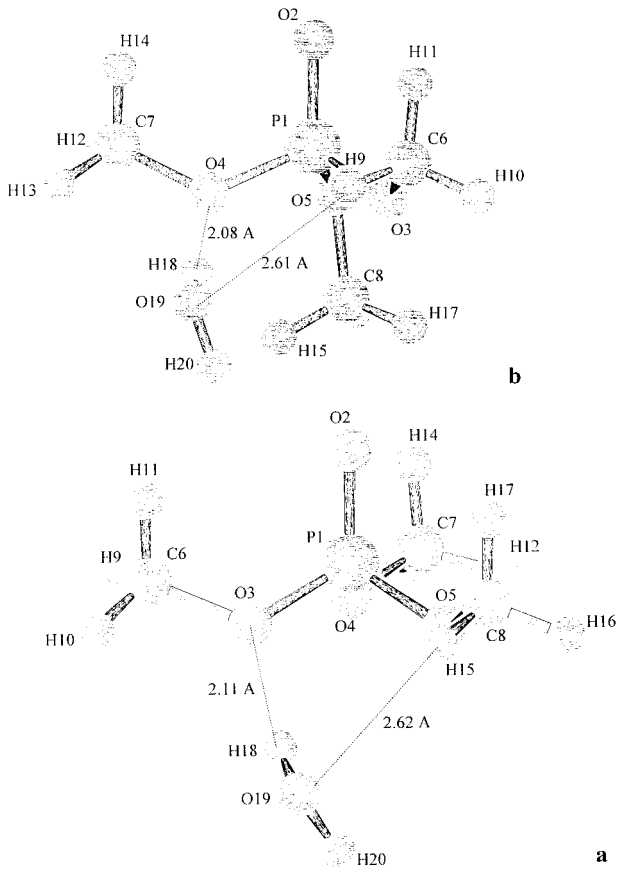

Figure 9. Structure of the (a) TMP(C_3)−H_2O alkoxy complex and (b) TMP(C_1)−H_2O alkoxy complex, showing selected bond distances.

The C_3 symmetry of the TMP submolecule implies that two more equivalent minima should exist for the complex discussed above; with the H_2O involved in a weak interaction with the two other methyl groups in a similar fashion.

TMP(C_1)−H_2O Phosphoryl Complex. Two minima, corresponding to two near-equivalent structures of the TMP(C_1)−H_2O phosphoryl complexes were obtained, the structures of which are shown in Figure 8. We will refer to the structure shown in Figure 8a as TMP(C_1)−H_2O (I) complex and that shown in Figure 8b as TMP(C_1)−H_2O (II) complex. Given the low symmetry (C_1) of this TMP conformer, we consider the two minima distinct. The two structures could not, however, be individually identified in our experiments. As in the TMP-(C_3)−H_2O complex, dual interaction sites were involved in these complexes, as shown by charge density and interatomic distance considerations. The net atom charge densities for these complexes are shown in Table 2.

TMP(C_3)−H_2O Alkoxy Complex. Figure 9a shows the structure of the TMP−H_2O complex where the H_2O was bonded to the *alkoxy oxygen* in TMP, with the TMP in the C_3 conformation. As in the phosphoryl oxygen-bonded complexes, there appears to be a dual interaction in the alkoxy complexes too. One is the H18−O3 interaction, with the interatomic distance for this pair of atoms being 2.10 Å. Changes in charge densities on these atoms following complex formation corroborates an interaction (Table 2). In addition we also note that the O19−H15 distance is 2.62 Å, which is just about the sum of the van der Waals radii for this pair of atoms. Charge density considerations imply an interaction between these atoms. Considering the C_3 symmetry of the TMP submolecule, we note that two more such equivalent minima should exist, where the H_2O interacts with each of the other two alkoxy oxygens and

TABLE 1: Selected Structural Parameters and Dipole Moments for the Various TMP−H_2O Complexes Calculated at the HF/6-31G Level**

parameter[a]	TMP(C_3)−H_2O (phosphoryl)	TMP(C_1)−H_2O (I) (phosphoryl)	TMP(C_1)−H_2O (II) (phosphoryl)	TMP(C_3)−H_2O (alkoxy)	TMP(C_1)−H_2O (alkoxy)
H18−O2	1.9675	1.9598	1.9704		
H18−03				2.1048	
H18−04					2.0777
O19−H14	2.5291	2.5290			
O19−H11			2.5024		
O19−H15				2.6200	
O19−H9					2.6125
∠H18−O2−P1	131.1	132.8	129.3		
∠H18−O3−P1				117.4	
∠H18−O4−P1					120.8
∠O19−H18−O2	164.6	165.2	163.4		
∠O19−H18−O3				169.1	
∠O19−H18−O4					169.9
tor ∠H18−O2−P1O3[b]	−153.2	−101.9	−24.6		
tor ∠O19−H18−O2−P1	36.5	−40.0	22.0		
tor ∠H20−O19−H18−O2	92.1	−102.9	95.9		
tor ∠H18−O3−P1−O2				−122.9	
tor ∠O19−H18−O3−P1				49.9	
tor ∠H20−O19−H18−O3				−117.2	
tor ∠H18−O4−P1−O2					−115.4
tor ∠O19−H18−O4−P1					78.3
tor ∠H20−O19−H18−O4					−158.7
dipole moment (D)	2.5	3.8	4.2	2.6	4.2

[a] Bond lengths in angstroms. Angles in degrees. [b] Torsional angles ABCD between planes ABC and BCD; values positive for clockwise rotation about BC and viewed toward C.

TABLE 2: Net Atomic Charges on the Various Atoms of the TMP−H_2O Complexes[a]

atom	TMP(C_3)−H_2O phosphoryl	TMP(C_1)−H_2O (I) phosphoryl	TMP(C_1)−H_2O (II) phosphoryl	TMP(C_3)−H_2O alkoxy	TMP(C_1)−H_2O alkoxy
			TMP		
P1	**1.6709** (1.6431)	**1.7031** (1.6768)	**1.7018** (1.6768)	1.6564 (1.6431)	1.6992 (1.6768)
O2	**−0.7782** (−0.7395)	**−0.7502** (−0.7107)	**−0.7515** (−0.7107)	−0.7326 (−0.7395)	−0.7058 (−0.7107)
O3	−0.6825 (−0.6856)	−0.6995 (−0.7031)	−0.7030 (−0.7031)	**−0.7252** (−0.6856)	−0.7176 (−0.7031)
O4	−0.6859 (−0.6855)	−0.7268 (−0.7269)	−0.7242 (−0.7269)	−0.6848 (−0.6855)	**−0.7659** (−0.7269)
O5	−0.6850 (−0.6855)	−0.6776 (−0.6803)	−0.6780 (−0.6803)	−0.6978 (−0.6855)	−0.6797 (−0.6803)
C6	−0.0347 (−0.0340)	−0.0392 (−0.0346)	**−0.0580** (−0.0346)	−0.0345 (−0.0340)	**−0.0537** (−0.0346)
C7	**−0.0563** (−0.0340)	**−0.0511** (−0.0321)	−0.0328 (−0.0321)	−0.0359 (−0.0340)	−0.0349 (−0.0321)
C8	−0.0350 (−0.0340)	−0.0357 (−0.0328)	−0.0354 (−0.0328)	**−0.0531** (−0.0340)	−0.0345 (−0.0328)
H9	0.1345 (0.1314)	0.1381 (0.1311)	0.1325 (0.1311)	0.1352 (0.1314)	**0.1586** (0.1311)
H10	0.1424 (0.1391)	0.1431 (0.1401)	0.1393 (0.1401)	0.1441 (0.1391)	0.1388 (0.1401)
H11	0.1459 (0.1479)	0.1504 (0.1502)	**0.1789** (0.1502)	0.1557 (0.1479)	0.1528 (0.1502)
H12	0.1350 (0.1314)	0.1209 (0.1249)	0.1264 (0.1249)	0.1327 (0.1314)	0.1296 (0.1249)
H13	0.1394 (0.1391)	0.1370 (0.1345)	0.1385 (0.1345)	0.1416 (0.1391)	0.1405 (0.1345)
H14	**0.1727** (0.1479)	**0.1779** (0.1531)	0.1540 (0.1531)	0.1495 (0.1479)	0.1614 (0.1531)
H15	0.1327 (0.1314)	0.1303 (0.1277)	0.1293 (0.1277)	**0.1611** (0.1314)	0.1230 (0.1277)
H16	0.1431 (0.1391)	0.1443 (0.1414)	0.1440 (0.1414)	0.1371 (0.1391)	0.1455 (0.1414)
H17	0.1490 (0.1478)	0.1429 (0.1409)	0.1434 (0.1409)	0.1485 (0.1478)	0.1420 (0.1409)
			H_2O		
H18	**0.3861** (0.3353)	**0.3868** (0.3353)	**0.3874** (0.3353)	**0.3740** (0.3353)	**0.3743** (0.3353)
O19	**−0.7184** (−0.6707)	**−0.7203** (−0.6707)	**−0.7187** (−0.6707)	**−0.7035** (−0.6707)	**−0.7035** (−0.6707)
H20	0.3244 (0.3353)	0.3255 (0.3353)	0.3260 (0.3353)	0.3315 (0.3353)	0.3299 (0.3353)

[a] The net atomic charges on the atoms for the uncomplexed species are given in parentheses.

an adjacent methyl group; giving a total of three equivalent structures for the alkoxy oxygen bonded TMP(C_3)-H_2O complex.

TMP(C_1)−H_2O Alkoxy Complex. The corresponding alkoxy oxygen-bonded complex for the TMP(C_1) submolecule was also indicated by our computations (Figure 9b). However, unlike in the TMP(C_3)−H_2O alkoxy complex, only one minimum could be obtained in the TMP(C_1)−H_2O alkoxy complex, with the water being hydrogen bonded to the oxygen O4. We did try a starting geometry where the H_2O was located on the oxygens, O5 and O3. No minimum could be obtained in these cases.

Stabilization Energies. The stabilization energies of the different complexes calculated at different levels of theory are shown in Table 3. The stabilization energies were corrected for zero-point energies (ZPE) and for ZPE+BSSE as well. When correcting for ZPE, the computed ZPE were scaled by 0.9, because this factor brings the computed frequencies in approximate agreement with experimental values.[12]

At the HF/6-31G**//HF/6-31G** level, the ZPE+BSSE corrected stabilization energy for the TMP(C_3)−H_2O phosphoryl complex was 4.7 kcal/mol, while for both the TMP(C_1)−H_2O phosphoryl complexes (I and II), the stabilization energies were 5.0 kcal/mol. At the MP2//HF level, there was only a marginal difference, with all the three complexes referred to above having stabilization energies of ≈5 kcal/mol.

The ZPE+BSSE corrected stabilization energy of the TMP(C_3)−H_2O alkoxy complex was 1.8 kcal/mol at the HF level, which is significantly smaller than the values for the phosphoryl

TABLE 3: Stabilization Energies (kcal/mol) for the Various TMP−H_2O Complexes

corrected for	TMP(C_3)−H_2O (phosphoryl)	TMP(C_1)−H_2O (I) (phosphoryl)	TMP(C_1)−H_2O (II) (phosphoryl)	TMP(C_3)−H_2O (alkoxy)	TMP(C_1)−H_2O (alkoxy)
ZPE (HF)[a]	6.3	6.5	6.6	3.3	2.8
ZPE (MP2)[b]	8.0	8.2	8.4	5.8	5.4
ZPE+BSSE (HF)[a]	4.7	5.0	5.0	1.8	1.3
ZPE+BSSE+Reorg[c] (HF)[a]	4.5	4.7	4.8	1.5	1.0
ZPE+BSSE (MP2)[b]	4.9	5.0	5.1	2.6	2.3

[a] Level of theory used: HF/6-31G**/HF/6-31G**. [b] Level of theory used: MP2/6-31G**//HF/6-31G**. [c] "Reorg" refers to the energy correction for the reorganization of the monomer in the complex.

TABLE 4: Experimental and Computed Vibrational Frequencies (Scaled), Scaling Factors, and Assignments for the Various TMP−H_2O Complexes

ν (cm^{-1}) experiment	ν (cm^{-1}) calculated	scaling factor	mode assignmnet
1262	1264	0.919	$\nu_{P=O}$ in TMP(C_3)−H_2O complex[a]
[c]	1289, *1288*[d]	0.919	$\nu_{P=O}$ in TMP(C_1)−H_2O complex[a]
1292	1291	0.919	$\nu_{P=O}$ in TMP(C_3)−H_2O complex[b]
	1315	0.919	$\nu_{P=O}$ in TMP(C_1)−H_2O complex[b]
870	869, 871	0.925	$\nu_{(P-O)-C}$ in TMP(C_3)−H_2O complex[a]
857,870	855,*854*, 868, *867*	0.925	$\nu_{(P-O)-C}$ in TMP(C_1)−H_2O complex[a]
857	855, 865	0.925	$\nu_{(P-O)-C}$ in TMP(C_3)−H_2O complex[b]
	837, 861	0.925	$\nu_{(P-O)-C}$ in TMP(C_1)−H_2O complex[b]
1050, 1052	1042, 1049	0.884	$\nu_{P-(O-C)}$ in TMP(C_3)−H_2O complex[a]
1039, 1065	1036, *1037*, 1058, *1056*	0.884	$\nu_{P-(O-C)}$ in TMP(C_1)−H_2O complex[a]
1031, 1039	1033, 1040	0.884	$\nu_{P-(O-C)}$ in TMP(C_3)−H_2O complex[b]
	1025, 1052	0.884	$\nu_{P-(O-C)}$ in TMP(C_1)−H_2O complex[b]
3460, 3470	3559	0.876	ν_1 of H_2O in TMP(C_3)−H_2O complex[a]
3460, 3470	3560, *3561*	0.876	ν_1 of H_2O in TMP(C_1)−H_2O complex[a]
	3615	0.876	ν_1 of H_2O in TMP(C_3)−H_2O complex[b]
	3611	0.876	ν_1 of H_2O in TMP(C_1)−H_2O complex[b]
	3695	0.874	ν_3 of H_2O in TMP(C_3)−H_2O complex[a]
	3694, *3694*	0.874	ν_3 of H_2O in TMP(C_1)−H_2O complex[a]
	3708	0.874	ν_3 of H_2O in TMP(C_3)−H_2O complex[b]
	3709	0.874	ν_3 of H_2O in TMP(C_1)−H_2O complex[b]
1619	1629	0.902	ν_2 of H_2O in TMP(C_3)−H_2O complex[a]
1619	1629, *1628*	0.902	ν_2 of H_2O in TMP(C_1)−H_2O complex[a]
	1613	0.902	ν_2 of H_2O in TMP(C_3)−H_2O complex[b]
	1609	0.902	ν_2 of H_2O in TMP(C_1)−H_2O complex[b]

[a] Phosphoryl oxygen bonded complex. [b] Alkoxy oxygen bonded complex. [c] Features not observed experimentally. [d] Normal font refers to features of the TMP(C_1)−H_2O (I) complex; italics refer to the features of the TMP(C_1)−H_2O (II) complex.

oxygen bonded complexes. The corresponding value for the TMP(C_1)−H_2O alkoxy complex was 1.3 kcal/mol. At the MP2//HF level, the stabilization energies were 2.6 and 2.3 kcal/mol, for the C_3 and C_1 complexes, respectively.

It must be noted that when forming the complex, the TMP and H_2O submolecules undergo a small structural reorganization. When the full counterpoise correction was done using the procedure described by Mayer and Surjan,[18] to account for the changes in the structures of the submolecules, the stabilization energies of the complexes calculated at the HF level, decreased by ≈0.3 kcal/mol as shown in Table 3.

Vibrational Assignments. Table 4 gives the experimentally observed frequencies together with the computed values for the various TMP−H_2O complexes optimized at the HF/6-31G** level. The computed frequencies were scaled on a mode-by-mode basis, as discussed in our earlier work.[12] The scaling factors for the different modes were determined by comparing the computed frequencies for a given mode in the uncomplexed submolecule with the corresponding experimental values. The scaling factors for the different modes are listed in Table 4.

Figures 1−3 show the experimentally observed features of the P═O and P−O−C modes in the TMP−H_2O complexes, together with a stick spectrum depicting the scaled computed frequencies. A comparison of the computed frequencies with the experimentally observed features led to the following assignments.

P═O Stretch in TMP in the TMP−H_2O Complex. The 1262 cm^{-1} feature (Figure 1 and Table 4) was assigned to the P═O stretch of the TMP submolecule in the TMP(C_3)−H_2O phosphoryl complex. The corresponding feature in the TMP(C_1)−H_2O phosphoryl complex, computed to occur at ≈1288 cm^{-1}, could not be discerned because it probably overlaps with the strong feature of uncomplexed TMP(C_3), which occurs at 1287 cm^{-1}.

For the alkoxy oxygen bonded complexes, our computations indicated the P═O stretching frequency of TMP to be blue shifted relative to the feature in the uncomplexed molecule. The feature at 1292 cm^{-1} was therefore assigned to the P═O stretch in TMP(C_3)−H_2O alkoxy complex. This assignment agreed well with the computed value for this mode in the corresponding complex. It is noteworthy that the alkoxy oxygen bound complex was observed experimentally only with the TMP in the C_3 conformation. No feature to the blue of the P═O stretch of free TMP in the C_1 conformer (i.e., to the blue of the 1305 cm^{-1} doublet) was observed that could be assigned to the TMP-(C_1)−H_2O alkoxy complex. It may be recalled that our calculations had shown that three equivalent structures exist for TMP(C_3)−H_2O alkoxy complex. However, only one stable structure was indicated for the TMP(C_1) case, which probably makes it less likely to observe the TMP(C_1)−H_2O alkoxy complex.

In our earlier work on the complexes of triethyl phosphate (TEP) with H_2O, we observed no alkoxy oxygen bound complexes.[9] We rationalized that observation by noting that the steric inhibition offered by the three ethyl groups in TEP probably prevented the formation of such a complex. The observation of the alkoxy oxygen bound complex in TMP, where the steric inhibition can be expected to be less than in TEP, supports our earlier rationalization. Hydrogen-bonded complexes involving the alkoxy oxygen were also observed in carboxylic acid ester−water systems, as in methyl acetate−water complexes.[6,7]

The red shift observed in the phosphoryl oxygen bonded complexes can be correlated with the 0.4% increase in the P═O bond lengths in these complexes relative to the bond lengths in uncomplexed TMP. Similarly the blue shift observed in the alkoxy oxygen bonded complex correlates well with the marginally shortened P═O bond length (<0.1%), computed in this complex.

(P−O)−C Stretch in TMP in the TMP−H_2O Complex. The new feature that emerged at 870 cm^{-1} when H_2O was co-deposited with TMP (Figure 2) was assigned to the (P−O)−C stretch of TMP in the TMP(C_3)−H_2O phosphoryl complex. As can be seen from Table 4, the computed/scaled frequency agreed well with the experimentally observed value. The (P−O)−C stretching mode occurs as a doubly degenerate mode in the

TMP(C_3) conformation. Our computations indicate that the double degeneracy of this mode is weakly lifted in the TMP-(C_3)−H_2O complex. However, the splitting in this mode (2 cm^{-1}) as a result of the lifting of the degeneracy is too small to be experimentally discerned.

Another spectral feature that increased in intensity with increase in H_2O concentration was the 857 cm^{-1} feature. On the basis of our computations, the 857 cm^{-1} feature along with the 870 cm^{-1} feature was assigned to the same mode in the TMP(C_1)−H_2O phosphoryl complex. The perturbations in the (P−O)−C modes of the TMP(C_1)−H_2O complex provided evidence for its formation. It must be recalled that the perturbation in the P═O mode for this complex was obscured by the strong feature due to monomeric TMP(C_3).

The features due to the TMP(C_3)−H_2O alkoxy complex were computed to occur at 857 and 866 cm^{-1}. The strong feature at 857 cm^{-1} can therefore be assigned to this complex. The 866 cm^{-1} feature is likely to be masked by the feature due to the monomeric TMP(C_3). Here again, the double degeneracy of the (P−O)−C stretching mode has been split in the TMP(C_3) submolecule in the TMP(C_3)−H_2O alkoxy complex as a result of complex formation. No feature that could be assigned to the TMP(C_1)−H_2O alkoxy complex could be discerned.

P−(O−C) Stretch in TMP in the TMP−H_2O Complex. As seen from Table 4 and Figure 3, a number of new features were observed in this region that were assigned to the TMP−H_2O complex. The features at 1039 and 1050/1052 cm^{-1} were assigned to the TMP(C_3)−H_2O phosphoryl complex, while the features at 1039 and 1065 cm^{-1} to the TMP(C_1)−H_2O phosphoryl complex.

The features at 1031 and 1039 cm^{-1} can be assigned to the TMP(C_3)−H_2O alkoxy complex.

With the P−(O−C) stretching mode also, our computations indicate that the double degeneracy in the C_3 conformation in the TMP(C_3)−H_2O complexes is lifted following complex formation. It must be admitted that the vast number of spectral features in this region shifted marginally from each other led to multiply assigned spectral features.

O−H Stretch in H_2O in the TMP−H_2O Complex. While the agreement between the calculated and experimental frequencies are good for the modes involving TMP, the agreement is far from satisfactory for the modes involving the O−H vibrations. It can be seen from Table 4, that the experimentally observed frequencies of the O−H stretch of H_2O in TMP−H_2O complexes, at 3460 and 3470 cm^{-1}, are red shifted from the ν_1 stretch in uncomplexed H_2O by ≈170 cm^{-1}. However, the corresponding computed shifts (≈70 cm^{-1}) are lower by more than a factor of 2.

While the agreement is poor for this mode, it is interesting that O−H stretches in hydrogen-bonded complexes are generally poorly represented when the frequency calculations are done at the HF level. Zhang et al. in their work on acetone−water complexes have observed similar disagreements between their computed and experimental shifts in the O−H stretches.[3] Kim et al. also report a disagreement by a factor of 2 in the O−H stretch in acetone−methanol complexes.[2] More recently Van Bael et al. in their work on imidazole complexes with water have shown that the vibrational shifts in the ν_1 mode of H_2O was experimentally observed to be 244 cm^{-1}, whereas at the HF/6-31G** level, the computed shifts were 84 cm^{-1}.[1] However, at the MP2/6-31G** and DFT/B3LYP/6-31G** levels, the computed shifts were 134 and 161 cm^{-1}, respectively, in better agreement with experiments than the HF values. Frequency calculations incorporating electron correlation are therefore necessary to predict the O−H stretching modes in hydrogen-bonded complexes. The TMP−H_2O system was inconveniently large for us to do frequency calculations incorporating electron correlation.

Our computations indicate that the frequencies of the ν_1 mode of H_2O in the TMP−H_2O phosphoryl complexes, corresponding to both conformers of TMP, are almost identical (Table 4). The closely lying features at 3460 and 3470 cm^{-1} can therefore be attributed to the phosphoryl oxygen bound complexes in which the TMP submolecule is in the C_3 and C_1 conformations. Given the large difference between the computed and experimental values, it was not possible for us to associate each of the two spectral features with a definite conformation of the TMP submolecule.

The perturbation in the ν_1 mode of H_2O in the *alkoxy* oxygen bound complex was computed to be 20 cm^{-1}, which is considerably smaller than that computed for the *phosphoryl* oxygen bound complex. Experimentally, however, we have not been able to identify the feature corresponding to this mode in the complex.

The ν_3 mode of H_2O was computed to be shifted by only 20 cm^{-1} in these complexes. The perturbation in this mode could not be discerned since they were probably masked by the features due to the self-associated complexes of H_2O.

O−H Bend in H_2O in the TMP−H_2O Complex. The bending mode ν_2 is computed to be blue shifted by about 32 cm^{-1} in the complex, relative to the frequency in uncomplexed H_2O, in the phosphoryl oxygen bound complexes involving both the C_3 and C_1 conformers of TMP. The assignment of our experimentally observed feature at 1619 cm^{-1} to this mode is therefore in reasonable agreement with the computed value. This experimental value differs from the computed/scaled value by a factor of 1.45. There appears to be a better agreement between the computed and experimental values for the ν_2 mode than for the ν_1, an observation that is in agreement with the findings in the acetone−water study.[2] The frequency for the alkoxy oxygen bonded complexes is computed to be blue shifted by 16 cm^{-1} for the TMP(C_3)−H_2O complex and 12 cm^{-1} for the TMP-(C_1)−H_2O adduct. Assuming that these values are high by the factor 1.45, the experimental frequencies can be expected to occur near 1608 and 1605 cm^{-1}, respectively. These features were however not observed being probably masked by the features due to the self-associated complexes of water.

TMP−D_2O Complexes. In experiments where TMP and D_2O were co-deposited, we found no discernible changes in the frequencies of the modes involving the TMP submolecule. Our computations also corroborated this observation. The ν_1 mode of D_2O was experimentally observed to occur at 2546 and 2552 cm^{-1} in the TMP−D_2O adduct, which amounts to a shift of 102 and 109 cm^{-1}, respectively, from the ν_1 mode of free D_2O. As with TMP−H_2O complexes, this shift is almost twice the computed shifts; the computed shifts being ≈50 cm^{-1}.

The computed $\Delta\nu/\nu$ for the TMP−H_2O complex was 0.020, while for the TMP−D_2O complex the ratio was 0.022. Experimentally the ratio for the TMP−H_2O and TMP−D_2O complexes were ≈0.05 and ≈0.04, respectively.

Conclusions

We have experimentally observed hydrogen-bonded complexes of TMP and H_2O trapped in a nitrogen matrix. Two classes of complexes were observed: one in which the H_2O was bonded to the phosphoryl oxygen and another where the

bonding was at the alkoxy oxygen of TMP. Given that TMP itself exists in two different conformations, a number of complexes were observed. Our computations indicated five distinct minima; though for reasons of symmetry of the C_3 conformer, a few more equivalent structures should exist. Experimentally we observed the phosphoryl oxygen bound TMP(C_3)−H_2O and TMP(C_1)−H_2O complexes, and the alkoxy oxygen bound TMP(C_3)−H_2O complex. The formation of these complexes was evidenced by perturbations in the modes of both TMP and H_2O submolecules. Given the multiplicity of the TMP−H_2O adducts, a number of vibrational features are multiply assigned. However, the appearance of the product bands in good agreement with the computed values lends support to our assignment. In particular, we would also like to highlight that the formation of certain complexes was experimentally confirmed by vibrational features that were *uniquely* assigned to these complexes. The 1262 cm^{-1} feature uniquely assigned to the TMP(C_3)−H_2O phosphoryl complex confirmed its presence, while the 1292 cm^{-1} feature provides evidence for the occurrence of the alkoxy oxygen bound TMP(C_3)−H_2O complex.

Ab initio computations at the HF/6-31G** level were performed to rationalize the experimental observations. While the computed frequencies agreed well for the modes involving the TMP submolecule, a discrepancy amounting to a factor of 2 was observed for the shifts in the mode for the H_2O submolecule.

Stabilization energies for the various complexes were computed at the HF/6-31G** level and using single-point calculations at the MP2/6-31G** level. The phosphoryl oxygen bonded complexes, with a binding energy of about 5 kcal/mol, were stronger than the alkoxy oxygen bonded complex, the stabilization energy of which was only ≈2 kcal/mol.

An aspect of our study which we find interesting is that in every single TMP−H_2O complex, dual interaction sites were involved; one a hydrogen-bonded interaction between the hydrogen in water and the phosphoryl oxygen in TMP and another between the hydrogen in the methyl group of TMP and the oxygen in water. Such combined participation of dual hydrogen-bonded interactions in the determination of the structure of a supermolecule involving an organic phosphate may provide valuable insights in bonding aspects in biological systems, where organic phosphates can serve as models.

In this work, we have also shown that the supersonic jet source for matrix isolation spectroscopy can be used to address problems of matrix interactions.

Acknowledgment. A gift of a workstation to IIT, Chennai, from Alexander von Humboldt Foundation (Germany) is acknowledged with thanks. L.G. gratefully acknowledges the Research Fellowship awarded by the Council of Scientific and Industrial Research, India. V.V. acknowledges the award of a Research Fellowship from the Department of Atomic Energy, India.

References and Notes

(1) Van Bael, M. K.; Smets, J.; Schoone, K.; Houben, L.; McCarthy, W.; Adamowicz, L.; Nowak, M. J.; Maes, G. *J. Phys. Chem.* **1997**, *101*, 2397.

(2) Han, S. W.; Kim, K. *J. Phys. Chem.* **1996**, *100*, 17124.

(3) Zhang, X. K.; Lewars, E. G.; March, R. E.; Parnis, J. M. *J. Phys. Chem.* **1993**, *97*, 4320.

(4) Vandevyvere, P. J.; Maes, G.; Zeegers-Huyskens, Th. *Spectrosc. Lett.* **1987**, *20*, 461.

(5) (a) Barnes, A. J.; Bentwood, R. M.; Wright, M. P. *J. Mol. Struct.* **1984**, *118*, 97. (b) Andrews, L. *J. Mol. Struct.* **1983**, *100*, 281. (c) Paul, S. O.; Ford, T. A. *Spectrochim. Acta* **1988**, *44A*, 587. (d) DeLaat, A. M.; Ault, B. S. *J. Am. Chem. Soc.* **1987**, *109*, 4232. (e) Jeng, M. H.; Ault, B. S. *J. Phys. Chem.* **1990**, *94*, 1326. (f) Jeng, M. H.; Ault, B. S. *J. Phys. Chem.* **1990**, *94*, 4851. (g) Maes, G.; Smets, J. *J. Phys. Chem.* **1993**, *97*, 1818.

(6) Vanderheyden, L.; Maes, G.; Zeegers Huyskens, Th. *J. Mol. Struct.* **1984**, *114*, 165.

(7) Maes, G.; Zeegers Huyskens, Th. *J. Mol Struct.* **1984**, *100*, 305.

(8) George, L.; Sankaran, K.; Viswanathan, K. S.; Mathews, C. K. *Appl. Spectrosc.* **1994**, *48*, 7.

(9) George, L.; Sankaran, K.; Viswanathan, K. S.; Mathews, C. K. *Appl. Spectrosc.* **1994**, *48*, 801.

(10) George, L.; Sankaran, K.; Viswanathan, K. S.; Mathews, C. K. *Spectrochim. Acta* **1995**, *51A*, 801.

(11) Vidya, V.; Sankaran, K.; Viswanathan, K. S. *Chem. Phys. Lett.* **1996**, *258*, 113.

(12) George, L.; Viswanathan, K. S.; Singh, S. *J. Phys. Chem.* **1997**, *101*, 2459.

(13) Frisch, M. J.; Trucks, G. W.; Head-Gordon, M.; Gill, P. M. W.; Wong, M. W.; Foresman, J. B.; Johnson, B. G.; Schlegel, H. B.; Robb, M. A.; Replogle, E. S.; Gomperts, R.; Andres, J. L.; Raghavachari, K.; Binkley, J. S.; Gonzalez, C.; Martin, R. L.; Fox, D. J.; Defrees, D. J.; Baker, J.; Stewart, J. J. P.; Pople, J. A. Gaussian Inc.: Pittsburgh, PA, 1992.

(14) Boys, S. F.; Bernardi, F. *Mol. Phys.* **1970**, *19*, 553.

(15) Fredin, L.; Nelander, B.; Ribbegard, G. *J. Chem. Phys.* **1977**, *66*, 4065.

(16) Tursi, A. J.; Nixon, E. R. *J. Chem. Phys.* **1970**, *52*, 1521.

(17) Jabalameli, A.; Zhanpeisov, N. U.; Nowek, A.; Sullivan, R. H.; Leszezyynski, J. *J. Phys. Chem. A* **1997**, *101*, 3619.

(18) Mayer, I.; Surjan, P. R. *Chem. Phys. Lett.* **1992**, *191*, 497.